

A Confirmatory Approach for Integrating Neural and Behavioral Data into a Single Model

Don van Ravenzwaaij, Alexander Provost, and Scott D. Brown
University of Newcastle

Word count: 5,800

Correspondence concerning this article should be addressed to:

Don van Ravenzwaaij

University of Newcastle, Department of Psychology

University Drive, Aviation Building, room AVG11

Callaghan NSW 2308, Australia

Ph: (+61) 2-4921-5662

E-mail should be sent to don.vanravenzwaaij@newcastle.edu.au.

Abstract

Recent decades have witnessed amazing advances in both mathematical models of cognition and in the field of cognitive neuroscience. These developments were initially independent of one another, but recently the fields have started to become interested in joining forces. The resulting joint modeling of behavioral and neural data can be difficult, but has proved fruitful. We briefly review different approaches used in decision-making research for linking behavioral and neural data, and also provide an example. Our example provides a tight link between behavioral data and evoked scalp potentials measured during mental rotation. The example model illustrates a powerful hypothesis-driven way of linking such data sets. We demonstrate the use of such a model, provide a model comparison against interesting alternatives, and discuss the conclusions that follow from applying such a joint model.

Keywords: Joint Modeling; Cognitive Neuroscience; Response Time Data; ERP.

1 Like many areas of scientific enquiry, cognitive psychology began with verbally-
2 specified theories and gradually progressed to quantitative accounts over time. This resulted
3 in mathematical models to describe memory (e.g., Atkinson & Shiffrin, 1968; Raaijmakers
4 & Shiffrin, 1981), categorization (e.g., Nosofsky, 1986; Nosofsky & Palmeri, 1997), speeded

5 and unspeeded decision making (e.g., Ratcliff, 1978; Wagenmakers, 2009), and many other
6 paradigms (for reviews, see Lee & Wagenmakers, 2013; Lewandowsky & Farrell, 2010).
7 A separate and at first mostly unrelated development was the advent of cognitive neu-
8 roscience. This field sought to map changes in the brain as they related to cognition,
9 using neural measurements obtained through event-related potentials (ERPs; e.g., Sutton,
10 Braren, Zubin, & John, 1965; Hillyard, Hink, Schwent, & Picton, 1973), the magnetoen-
11 cephalogram (MEG; e.g., Brenner, Williamson, & Kaufman, 1975), functional magnetic
12 resonance imaging (fMRI; e.g., Belliveau et al., 1991), and single-unit recordings in non-
13 human primates (e.g., Hanes & Schall, 1996; Schall, 2001; Shadlen & Newsome, 1996). As
14 progressively more precise measures of the inner workings of the brain became available,
15 researchers have become increasingly capable at understanding the neural determinants of
16 cognitive processes.

17 Some research paradigms have well-specified and tractable mathematical models of
18 cognition, and also well-developed methods for neural measurement, for example, sim-
19 ple decision-making and reinforcement learning. Researchers interested in such paradigms
20 started investigating ways to link the neural and behavioral data more carefully. The lat-
21 est developments include so-called *joint models*, in which data of one kind can inform the
22 model fit of the other kind and vice versa (e.g., Purcell et al., 2010; Turner, Forstmann, et
23 al., 2013; Anderson & Fincham, 2014; Turner, Forstmann, Love, Palmeri, & van Maanen,
24 in press). These accounts aim for the most explicit and careful links, by simultaneously
25 modeling neural recordings and behavioral outputs, allowing both kinds of data to inform
26 model selection and parameter estimation. Joint modeling provides an important theoret-
27 ical contribution: it allows a researcher to examine common denominators underlying both
28 behavioral data and neural data.

29 In this paper, we provide an example of how to jointly model behavioral and neural
30 data from simple decision-making. As an illustrative example, we apply a joint model
31 of behavioral responses and EEG recordings to data from an experiment based on the
32 classic Shepard-Metzler mental rotation task (Shepard & Metzler, 1971). However, before
33 describing the model, we review different approaches to linking behavioral and neural data,
34 with a focus on decision-making research.

35 An important change in the development of decision-making models over the past
36 twenty years has been a steady “tightening” of the link between neural and behavioral data
37 (for reviews and discussion of linking behavioral and neural data, see Teller, 1984). Early
38 models of simple decision-making linked behavioral and neural data loosely, by constraining
39 the development of behavioral models to respect data from neural measurements. For exam-
40 ple, the leaky competing accumulator model developed by Usher and McClelland (2001) was
41 structurally constrained to include components supported by neural investigations, such as
42 lateral inhibition between accumulating units, and passive decay of accumulated evidence.
43 These links were included as part of the model development process, and thereafter there
44 was no further attempt to link neural with behavioral data.

45 Subsequent models tested the links via qualitative comparisons between predictions
46 for corresponding neural and behavioral data sets. This kind of linking was very common in
47 early research into decision-making with fMRI methods, in which predictions were based on
48 the assumption that an experimental manipulation will influence one particular model com-
49 ponent, which leads naturally to predictions for the behavioral data, and also for the neural

50 data (via the hypothesized link). Predictions most frequently take the form “in condition A
51 vs. B , behavioral measure X should increase while neural measure Y decreases”. Support
52 for the predictions is taken as evidence in favor of the model, including the hypothesized
53 link. As an example, Ho, Brown, and Serences (2009) tested predictions generated from
54 decision-making models via hypothesized neural links. In one part of their study, Ho et
55 al. manipulated the difficulty of a decision-making task and hypothesized that this should
56 result in a change in the speed of evidence accumulation in a sequential sampling model.
57 By examination of the model coupled to a standard model for haemodynamic responses,
58 Ho et al. generated predictions for the blood-oxygen-level dependent (BOLD) response
59 profile within regions that are involved in perceptual decision making. These predictions
60 were compared with data from an fMRI experiment, which lent support to some accounts
61 over others.

62 Linking via the testing of qualitative hypotheses was later surpassed by quantitative
63 approaches, which provided a tighter link between neural and behavioral data. The most
64 common example of quantitative linking in decision-making models takes parameters of the
65 decision-making model, estimated from behavioral data, and compares them against the
66 parameters of a descriptive model estimated from the neural data. For example, Forstmann
67 et al. (2008) correlated individual subjects’ model parameters, estimated from behavioral
68 data, against blood-oxygen-level dependent (BOLD) parameter estimates; subjects with
69 large changes in threshold parameters also showed similarly large changes in BOLD re-
70 sponses.

71 Most recently, there have been efforts to link neural and behavioral decision-making
72 data even more tightly, by combining both data sets in a single model-based analysis. This
73 approach has culminated in models such as that developed by Purcell et al. (2010) which uses
74 neural measurements as a model input in order to predict both behavioral measurements
75 and a second set of neural measurements. This provides a simultaneous description of neural
76 and behavioral data sets, as well as explicating the links between them. A less detailed, but
77 more general approach was developed by Turner, Forstmann, et al. (2013) and extended
78 by Turner et al. (in press) in this volume. In their method, neural and behavioral models
79 are joined by allowing their parameters to covary. Turner, Forstmann, et al.’s approach is
80 a “joint” model, in the sense that it allows symmetric information flow: behavioral data
81 can influence the neural parameter estimates, and neural data can influence the behavioral
82 parameter estimates. This information flow is achieved via a covariance matrix for the model
83 parameters. This structure allows the identification of covariance between model parameters
84 associated with neural processes and model parameters associated with behavioral processes.
85 However, Turner, Forstmann, et al.’s approach differs from our analyses in its focus. The
86 covariance matrix of Turner, Forstmann, et al.’s approach means that any and all parameters
87 of the behavioral model are allowed to link with any and all parameters of the neural model,
88 although all these links are required to be linear. Our approach is less general, but more
89 pointed, because it requires the specific instantiation of a single, precise link between one
90 parameter of the neural model and one parameter of the behavioral model.¹

91 The joint modeling approach of Turner, Forstmann, et al. (2013) is complementary

¹While it is true that Turner, Forstmann, et al.’s method could, in theory, be restricted to produce our approach (e.g. by setting almost all priors on the covariance matrix components to zero, and by adding in nonlinear parameter link functions) in practice this has not been done.

92 to the approach we use. For paradigms in which there exist precise hypotheses about the
93 links between neural and behavioral models, our approach offers a straightforward way of
94 instantiating and testing these hypotheses. For paradigms in which this is not the case,
95 Turner, Forstmann, et al.’s approach offers a powerful tool for exploration. What both
96 approaches have in common is that they *jointly* fit the neural and behavioral data, which
97 allows behavioral data to influence parameters on the “neural side” of the model, and vice
98 versa. A joint model in this sense is able to identify a compromise between the two streams
99 of data. This means that, compared to an otherwise-identical model that is fit solely to the
100 behavioral (or neural) data, a joint model will always fit more poorly. Coherently managing
101 the compromise between fitting neural and behavioral data streams is a strength of the joint
102 modeling approach. For example, suppose one was examining a joint model for behavioral
103 and neural data, but was not fitting the model in a “joint” manner. Instead, imagine the
104 model was examined by fitting first to behavioral data alone, and then later evaluating the
105 model by comparing its subsequent predictions for neural effects against the neural data.
106 One problem with this approach arises if the model had two sets of parameters (say, A and
107 B) which both provided very good fits to the behavioral data, but very different fits to the
108 neural data. Suppose that parameter set A provided slightly better behavioral fits, but also
109 terrible neural fits, while parameter set B provided good fits to the neural data. Fitting to
110 the behavioral data alone would lead the researcher to choose parameter set A, and then to
111 reject the model because of the terrible fit to neural data. Joint fitting allows identification
112 of compromise parameters (such as set B) which provide good fits to both data streams.

113 The two-stage approach to model evaluation, in which the flow of information between
114 the two types of data is mostly one-way, was employed by Purcell et al. (2010) (they used
115 two different neural data streams, only one of which was a fitting target). While we hope
116 that a joint modeling approach has some strengths that the two-stage approach does not,
117 Purcell et al.’s work included important other advantages that have been absent in the joint
118 modeling work to date. For example, Purcell et al.’s approach was used to conduct pointed
119 comparisons between competing hypotheses about both the underlying model structures,
120 and the hypothesized links between neural and behavioral data. While such comparisons
121 are, theoretically, possible in joint modeling approaches, they can be difficult to implement,
122 and have not been investigated to date. The joint model we describe below is an attempt
123 to combine the advantages of the confirmatory approach of Purcell et al. (2010) with the
124 sophisticated estimation approach of Turner, Forstmann, et al. (2013). Similar to Turner,
125 Forstmann, et al.’s approach, we employ a simultaneous estimation procedure. However,
126 our approach is confirmatory in that we test an explicit and pre-specified link between
127 neural and behavioral data. We fit both behavioral and neural data streams at the same
128 time. In the next section, we will describe the behavioral task as well as the two types of
129 data.

130 Data

131 The data we use are from an experiment based on the classic Shepard–Metzler *mental*
132 *rotation task* (Provost, Johnson, Karayanidis, Brown, & Heathcote, 2013). The mental
133 rotation task is a two-alternative forced choice task in which participants are asked to
134 examine a pair of stimuli, one of which is rotated relative to the other. Crucially, participants
135 are asked to indicate as quickly and accurately as possible whether the stimuli are identical

136 (“same”) or whether one is different from the other (“different”). For instance, in the left
 137 panel of Figure 1, the right stimulus is the same as the left stimulus. On the other hand,
 138 in the right panel of Figure 1, the right stimulus is the mirror-image of the left stimulus
 139 (“different”).

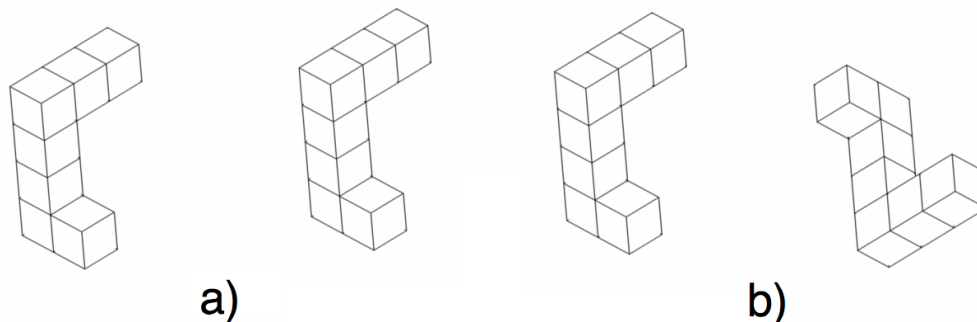


Figure 1. Two sample stimuli from Provost et al. (2013). Left panel: the right stimulus is the same as the left stimulus. Right panel: the right stimulus is different from the left stimulus.

140 The data we use here is from the first session of the first experiment reported by
 141 Provost et al. (2013). The experiment included five conditions that differed in the angle of
 142 rotation of the right stimulus: 0° , 45° , 90° , 135° , and 180° . The left stimulus was always
 143 identical to the one displayed in Figure 1.

144 Within each condition, half of the stimuli were “same” and half were “different”.
 145 The corresponding behavioral data were response times and choices from all conditions, for
 146 all participants. The neural data we will consider are mean amplitudes of single trials of
 147 the ERP signal corresponding to each trial used in the behavioral analysis. As in Provost
 148 et al. (2013), we report ERP effects from the midline parietal electrode site Pz, with a
 149 common average reference. Comparing mean amplitudes at Pz we are able to model a
 150 specific ERP modulation called “rotation related negativity” (RRN; Heil, 2002; Riečanský
 151 & Jagla, 2008), which is considered an index of mental rotation. Specifically, we look at
 152 increased mean amplitude negativity associated with increased angular displacement across
 153 8 epochs, from 200 to 1,000ms post stimulus onset in 100ms windows. For more details,
 154 please see the methods section of Experiment 1 and Figure 4 of Provost et al. (2013).

155 The use of sequential accumulator models for the analysis of response time data is not
 156 new (e.g., Link & Heath, 1975; Ratcliff, 1978; Wagenmakers, 2009). For these data, we turn
 157 to a relatively recent accumulator model: the Linear Ballistic Accumulator (LBA; Brown
 158 & Heathcote, 2008). An advantage of the LBA is tractability, as it has an easily-computed
 159 closed-form expression for its likelihood. As a result, it is relatively straightforward to
 160 expand the model to include a neural component. In the next section, we will introduce
 161 the reader to the behavioral and neural components of the model and demonstrate how we
 162 combine them into a joint model.

The Modeling

163

164 In the first sub-section below, we introduce the behavioral model. In the second
 165 sub-section, we introduce the neural modeling and the link between the two elements.

166 *The Behavioral Level: LBA*

167 In the LBA for multi-alternative RT tasks (Brown & Heathcote, 2008), stimulus
 168 processing is conceptualized as the accumulation of information over time. A response is
 169 initiated when the accumulated evidence reaches a predefined threshold. An illustration for
 170 two response options is given in Figure 2.

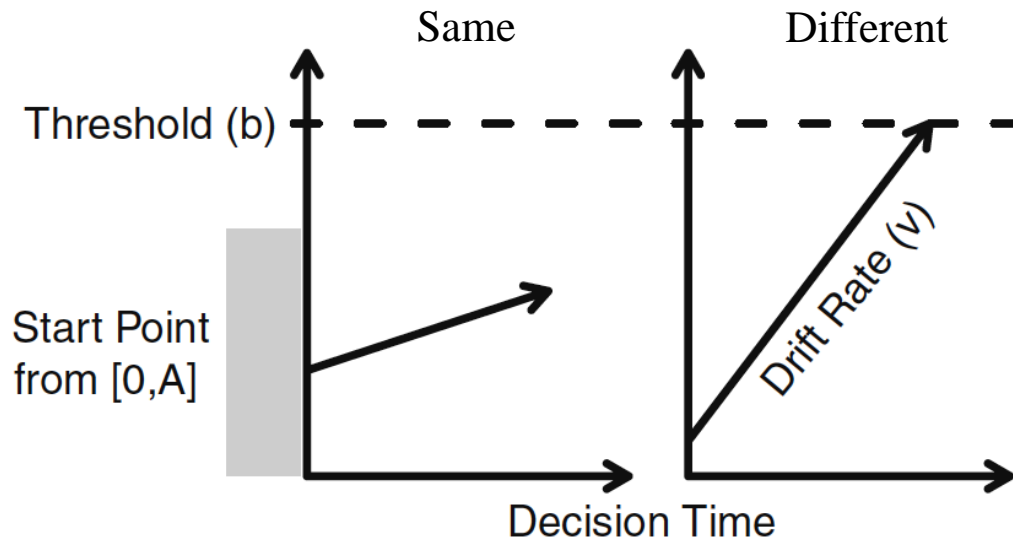


Figure 2. The LBA and its parameters for two response options (for this trial, the “different” response is the correct answer). Evidence accumulation begins at a start point drawn randomly from a uniform distribution with interval $[0, A]$. Evidence accumulation is governed by drift rate d , drawn across trials from a normal distribution with mean ν and standard deviation s . A response is given as soon as one accumulator reaches threshold b . Observed RT is an additive combination of the time during which evidence is accumulated and non-decision time t_0 .

171 The LBA assumes that the decision process starts from a random point between 0
 172 and A , after which information is accumulated linearly for each response option. The rate of
 173 this evidence accumulation is determined by drift rates d_1 and d_2 , normally distributed over
 174 trials with means ν_1 and ν_2 , and common standard deviation s . The distribution of drift

175 rates is truncated at zero to prevent negative accumulation rates. Threshold b determines
 176 the speed–accuracy tradeoff; lowering b leads to faster RTs at the cost of a higher error rate.

177 Together, these parameters generate a distribution of decision times DT . The ob-
 178 served RT, however, also consists of stimulus–nonspecific components such as response
 179 preparation and motor execution, which together make up non–decision time t_0 . The model
 180 assumes that t_0 simply shifts the distribution of DT , such that $RT = DT + t_0$ (Luce, 1986).
 181 Hence, the three key components of the LBA are (1) the speed of information processing,
 182 quantified by mean drift rate ν ; (2) response caution, quantified by boundary separation
 183 that averages to $b - A/2$; and (3) non–decision time, quantified by t_0 . The LBA has been
 184 successfully applied to a number of experimental paradigms including random dot motion
 185 tasks, brightness discrimination, consumer choice, and many others (e.g., Rae, Heathcote,
 186 Donkin, Averell, & Brown, 2014; Trueblood, Brown, & Heathcote, 2014; Ho, Brown, Abuyo,
 187 Ku, & Serences, 2012).

188 We specified the standard behavioral aspects of the LBA model using 24 parameters
 189 per participant for the 20 different response time distributions. The parameters included:
 190 one upper range of starting point A parameter, two parameters for threshold b (one each
 191 for “same” and “different” responses), ten parameters for both correct drift ν_c and for error
 192 drift ν_e (two stimuli types — “same”, “different” — times five angle conditions — 0° , 45° ,
 193 90° , 135° , 180°), and one non–decision time parameter t_0 . The 20 different response time
 194 distributions (and 10 free response probabilities) arose from factorial combination of two
 195 stimulus classes (same vs. different) with two response classes (same vs. different) and five
 196 rotation angles. This parameterization was chosen because it provides a reasonable com-
 197 promise between goodness-of-fit and tractability, as demonstrated in the extensive analyses
 198 of alternative models for data from a related experiment (Provost & Heathcote, 2015). Im-
 199 portantly, the evidence accumulators of the model have been linked to neural activity in
 200 the brain (e.g., Purcell et al., 2010; Gold & Shadlen, 2007). Because of this, mean drift rate
 201 ν lends itself naturally to be the driving parameter behind our ERP data.

202 We used a hierarchical Bayesian implementation of the LBA (Turner, Sederberg,
 203 Brown, & Steyvers, 2013). Advantages of the hierarchical Bayesian framework include
 204 the ability to fit the LBA to data with relatively few trials, because the model borrows
 205 strength from the hierarchical structure. The Bayesian set–up allows for using MCMC
 206 sampling, which is an efficient approach to parameter estimation (Gamerman & Lopes,
 207 2006; Gilks, Richardson, & Spiegelhalter, 1996; van Ravenzwaaij, Cassey, & Brown, in
 208 press). Starting points for the Markov chains were drawn from the following distributions:
 209 $A \sim N(2, 0.2)|(0,)$, both $bs \sim N(1, 0.1)|(0,)$, all ten $\nu_{cs} \sim N(3, 0.3)|(0,)$, all ten $\nu_{es} \sim$
 210 $N(1, 0.1)|(0,)$, and $t_0 \sim N(0.2, 0.02)|(0,)$. In this notation, $\sim N(x, y)|(0,)$ indicates that a
 211 parameter is normally distributed with mean x , standard deviation y , and is truncated to
 212 positive values only.

213 The hierarchical set–up prescribes that all individual parameters come from a trun-
 214 cated Gaussian group–level distribution. Thus, for each parameter to be estimated, we esti-
 215 mated a group level mean parameter and a group level standard deviation parameter. Priors
 216 for all group level mean parameters were normal distributions, with $A_\mu \sim N(2, 1)|(0,)$,
 217 both $b_\mu \sim N(2, 1)|(0,)$, all ten $\nu_{c\mu} \sim N(3, 1)|(0,)$, all ten $\nu_{e\mu} \sim N(1, 1)|(0,)$, and
 218 $t_{0\mu} \sim N(0.2, 0.1)|(0,)$. Priors for all group level standard deviation parameters were gamma
 219 distributions with a shape and a scale parameter of 1, except for $t_{0\sigma}$ which has a scale pa-

parameter of 3. Starting point distributions for group level μ were all identical to starting point distributions for the individual parameters, and starting point distributions for group level σ parameters were derived from starting point distributions for the individual parameters by dividing the mean by 10 and the standard deviation by 2. These prior settings are quite uninformative, and are based on previous experience with parameter estimation for the LBA model. As a result, the specific settings will not have a large influence on the shape of the posterior. For more details on distributional choices for the priors, we refer the reader to Turner, Sederberg, et al. (2013).

For sampling, we used 32 interacting Markov chains, and ran each for 1,000 burn-in iterations followed by 1,000 iterations after convergence. The two tuning parameters of the differential evolution proposal algorithm were set to standard values used in previous work: random perturbations were added to all proposals drawn uniformly from the interval $[-.001, .001]$; and the scale of the difference added for proposal generation was set to $\gamma = 2.38 \times (2K)^{-0.5}$, where K is the number of parameters per participant (24, in the model described above). The MCMC chains blocked proposals separately for each participant’s parameters, and also blocked the group-level parameters in $\{\mu, \sigma\}$ pairs.

Linking to Neural Data

The behavioral model above, based on the LBA, specifies a likelihood function for the response time data which gives the likelihood of observed data conditional on any given set of parameter values. This likelihood function supports all of our statistical analyses. The first step in bringing the neural data into the model is to define a likelihood function for the ERPs. We will assume that the ERP data, within any particular condition for any particular subject, are normally distributed. The next step is to link the parameters of the behavioral LBA model above with the parameters of the assumed normal model for the ERP data. To begin, we assume that the standard deviation of the normal distribution is fixed everywhere, for each subject, and that the mean of the normal distribution is given by an offset parameter (α) plus the drift rate parameter times a scale parameter (β):

$$ERP \sim N(\alpha + v \times \beta, \sigma) \quad (1)$$

The model is graphically displayed in Figure 3. Equation 1 provides a precise instantiation of the linking hypothesis in this joint model. Our very simple hypothesis is that the neural and behavioral data are linked via the drift rate parameter of the model, and that the link is a simple linear function. While simple to specify, this link has complicated implications. For example, the predicted ERP signal will change across conditions whenever drift rate changes – with rotation angle and with same vs. different stimulus pairings, in our experiment. The link also implies particular constraints on the model. For example, the drift rate parameter is forced to accommodate changes in both behavioral and neural data due to changes in rotation angle. The linking parameter serves as a time-sensitive measure of the link between behavioral and neural data. The model does more than just re-describe this link: the model attempts to capture the fact that different rotation angles cause different ERP measurements with a linking function and linking parameters that are identical for all angle conditions. As such, the model accounts for different ERPs across conditions entirely through drift rate.

For the neural data, we estimated one offset parameter α , one standard deviation parameter σ , and eight scale parameters β (one for each 100 ms epoch from 200 up to

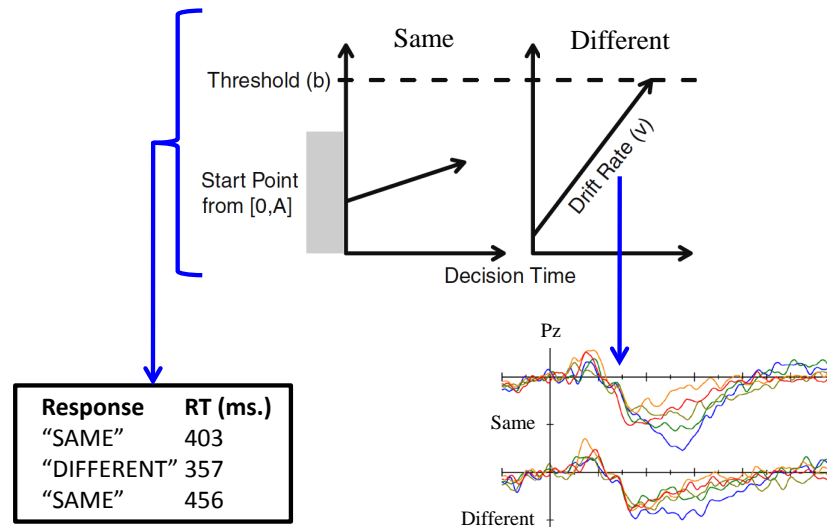


Figure 3. A symbolic display of the joint model. All LBA parameters inform the behavioral response data (bottom-left). The drift rate corresponding to the response given by the participant informs the ERP data (bottom-right).

262 1,000ms). The eight scale parameters allow investigation of how strongly the ERP signal is
 263 linked to cognition across the eight different time windows (200ms–300ms, 300ms–400ms,
 264 \dots , 900ms–1,000ms).

265 Starting points for the linking parameters were drawn from the following distribu-
 266 tions: $\alpha \sim N(8, 0.8)|(0,)$, all eight $\beta_s \sim N(1, 0.1)|(0,)$, and $\sigma \sim N(5, 0.5)|(0,)$. Analogous
 267 to the LBA parameters, all individual linking parameters were drawn from a truncated
 268 Gaussian group-level distribution. Priors for all group level mean parameters are normal
 269 distributions, with $\alpha_\mu \sim N(8, 2)|(0,)$, all eight $\beta_\mu \sim N(1, 1)|(0,)$, and $\sigma_\mu \sim N(5, 1)|(0,)$.
 270 Priors for all group level standard deviation parameters are gamma distributions with a
 271 shape and a scale parameter of 1. Starting point distributions for group level μ were all
 272 identical to starting point distributions for the individual parameters, and starting point
 273 distributions for group level σ parameters were derived from starting point distributions for
 274 the individual parameters by dividing the mean by 10 and the standard deviation by 2.

275 Data and code for the full model may be found on the web.²

²www.donvanravenzwaaij.com/Papers, and also at <https://osf.io/2r7bv/>.

276 *Model Comparison*

277 It is very difficult to judge model fit in an absolute sense. What constitutes a good
 278 fit, how much of a misfit is acceptable? In practice, it is almost always more fruitful to
 279 examine comparative goodness-of-fit, and to compare different models. We compare the
 280 model described above (henceforth ν -ERP) to three competing alternatives:

281 • t_0 -ERP: the behavioral parametrization is identical to that of ν -ERP, but the
 282 linking parameter to the neural data is non-decision time t_0 instead of drift rate ν (see e.g.
 283 Pouget et al., 2011, for corroborating evidence).

284 • *Brev- t_0 -ERP*: the behavioral parametrization for drift rates and non-decision time
 285 are reversed. In this model, we have one ν_c and one ν_e instead of ten each, and we have
 286 ten t_0 (one for each stimulus and angle condition) instead of one. Analogous to t_0 -ERP,
 287 the linking parameter to the neural data is non-decision time t_0 . Analogous to ν -ERP, the
 288 linking parameter to the neural data is now free to vary between stimuli types and angle
 289 conditions.

290 • ν -nonlinear-ERP: identical to the ν -ERP model, but testing a nonlinear link
 291 function between the drift rates and the ERP mean parameter. The nonlinear link function
 292 we test is the cumulative normal distribution function, which instantiates the hypothesis
 293 that scalp potentials might have important ceiling and floor effects. Such effects are plausible
 294 for many reasons, for example they may be imposed by physical and physiological limits on
 295 the electrical activity and conductivity of the cortex and scalp.

296 Priors and starting values were analogous for all four models.³ The models will be
 297 compared by visually inspecting the posterior predictives for obvious misfit. Numerically, we
 298 compare the models by calculating the Deviance Information Criterion (DIC; Spiegelhalter,
 299 Best, Carlin, & van der Linde, 2002), a measure which balances goodness of fit against
 300 model complexity. In this sense, DIC is similar to the well-known BIC and AIC measures,
 301 but DIC extends these by quantifying model complexity as across-sample variability in
 302 model fit rather than simply counting up the number of free parameters. As such, DIC
 303 usually assumes a stronger penalty for complexity. Lower values of DIC indicate better
 304 support for a model from the data.

305 Results

306 ν -ERP

307 As a first check of model fit, we compared posterior predictive data against the neural
 308 and behavioral data in Figure 4. The figure displays data averaged over participants with
 309 boxplots representing empirical data and lines representing synthetic data. The left two
 310 columns show model correspondence to the .1, .3, .5, .7, and .9 quantiles calculated from
 311 correct RTs (green) and error RTs (red). The right two columns show model correspondence
 312 to mean ERP amplitudes for each of the eight different time windows (200ms–300ms, 300ms–
 313 400ms, \dots , 900ms–1,000ms). The first and third column show model correspondence for
 314 “same” stimuli, the second and fourth column show model correspondence for “different”

³E.g., all ten t_0 used in the *Brev- t_0 -ERP* model have the same starting values and prior as the one t_0 used in the ν -ERP model; all ten ν_c used in the ν -ERP model have the same starting values and prior as the one ν_c used in the *Brev- t_0 -ERP* model.

315 stimuli. Rows show model correspondence for different rotation conditions (0° , 45° , 90° ,
 316 135° , 180°).

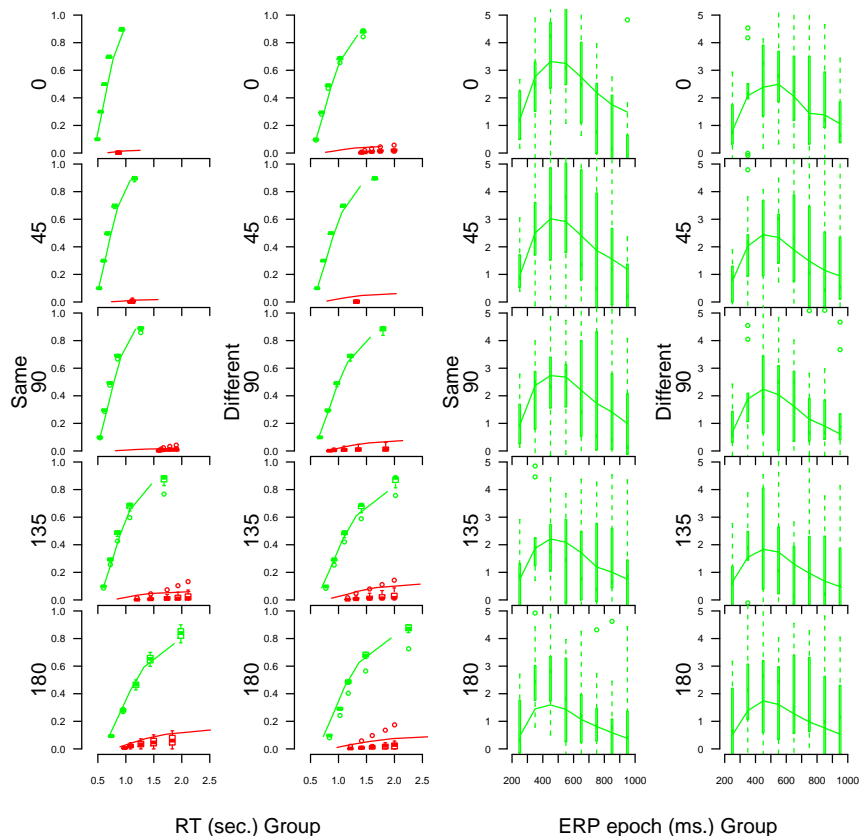


Figure 4. Posterior predictives show that the ν -ERP model fit both the behavioral data and the neural data well. Left two columns: proportion correct (y-axis) plotted against RTs (x-axis) for the .1, .3, .5, .7, and .9 quantiles calculated from correct RTs (green) and error RTs (red). Right two columns: mean ERP amplitudes in negative microvolts (y-axis) for eight different time windows (x-axis). For all panels, boxplots represent empirical data and lines represent posterior predictive data.

317 On the whole, the ν -ERP model fit both data sets well, although there is some misfit.
 318 The model captures the qualitative changes in RT distributions and percentage correct
 319 across same vs. different stimuli, and across the different angles of rotation. There is a
 320 tendency for the model to under-predict the accuracy in some conditions, as evidenced by
 321 the fact that the green lines are slightly lower than the center of the green boxplots and the
 322 red lines slightly higher than the center of the red boxplots. For the neural data, the model
 323 seems to capture the ERP distributions over time well. These conclusions about absolute,
 324 global model fit are necessarily vague, because of the previously mentioned difficulties in
 325 assessing absolute model fit. This is one of the reasons we turn to model comparison below.

326 The first model comparison we provide is to a behavioral-data-only version of the

327 ν -ERP model. The joint model must necessarily fit more poorly than the behavioral-only
 328 model, because the parameters of the joint model are further constrained to accommodate
 329 effects in the neural data (in a statistical sense, the behavioural-only model “nests” the
 330 behavioral side of the ν -ERP model). In order to examine this constraint, we compare the
 331 posterior predictives of our joint model fits to posterior predictives of a fit to the behavioral
 332 data alone. Parameter settings were as outlined in section “The Behavioral Level: LBA”.
 333 The posterior predictives for the behavioral-only model can be found in Figure 5.

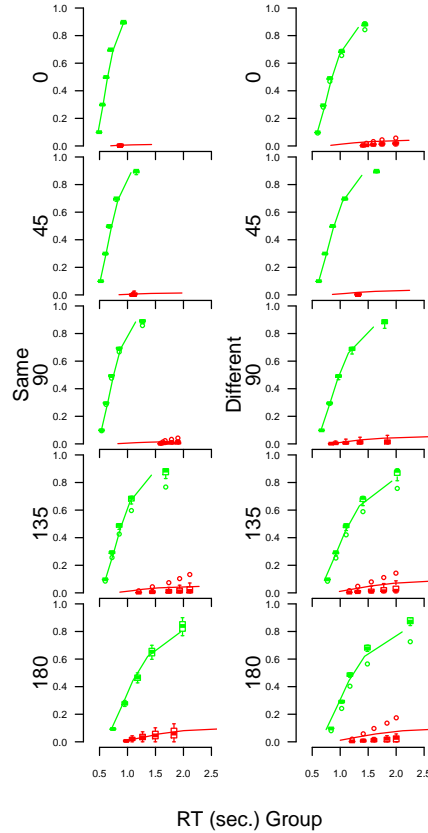


Figure 5. Posterior predictives show that the behavioral-only version of the joint ν -ERP model fit the behavioral data well. Displayed are the proportion correct (y-axis) plotted against RTs (x-axis) for the .1, .3, .5, .7, and .9 quantiles calculated from correct RTs (green) and error RTs (red). For both panels, boxplots represent empirical data and lines represent posterior predictive data.

334 Visual comparison of Figure 4 and Figure 5 shows that the model fit is almost identi-
 335 cal. The joint model compromises slightly on the accuracy fit compared to the behavioral-
 336 only model, but other than that, the models appear indistinguishable. To provide a sta-
 337 tistical comparison, the likelihood of the mean parameters averaged over all participants is
 338 -233.93 for the simple model. For the joint model, when selecting the behavioral component
 339 of the model and taking the likelihood of those mean parameters averaged over all partic-
 340 ipants, the value is -255.69, lending further credence to the observation that these models

341 fit the data comparably. It is not appropriate to compare these likelihood values further,
 342 e.g. by calculating DIC, because the likelihood of the behavioral data under the joint model
 343 does not satisfy the assumptions of those analyses, because of the conditioning on neural
 344 data.

345 We next examine a different, but plausible, candidate for the link between behavioral
 346 and neural data: the non-decision time parameter, t_0 . We do so by comparing two new
 347 models. The first has a behavioral parametrization which is identical to the original ν -ERP
 348 model, but has a link to the neural data through the t_0 parameter (this model is called
 349 t_0 -ERP). The second model corresponds to the original ν -ERP model but with the roles
 350 for non-decision time (t_0) and drift rate (ν) reversed (this model is called *Brev- t_0 -ERP*).

351 t_0 -ERP

352 Posterior predictive data for the t_0 -ERP model are shown in Figure 6. Visual in-
 353 spection of the figure shows that the t_0 -ERP model fits the behavioral data well, but does
 354 not capture the neural data as well as the ν -ERP model. This impression is supported by
 355 comparison of the DIC values for the two models: ν -ERP has an average DIC across partic-
 356 ipants of 31,880.75, whereas t_0 -ERP has an average DIC across participants of 31,909.18.
 357 Within participants, the ν -ERP model was DIC-preferred for 6 out of 9 people.

358 *Brev- t_0 -ERP*

359 Posterior predictive data for the *Brev- t_0 -ERP* model are shown in Figure 7. Visual
 360 inspection of the figure shows that the model fits the behavioral data worse than both other
 361 models. The *Brev- t_0 -ERP* model captures the neural data better than the t_0 -ERP model,
 362 but not as good as the ν -ERP model. Again, this impression is supported by analysis of
 363 DIC values: *Brev- t_0 -ERP* has an average DIC across participants of 32,039.64, worse than
 364 both other models. It is also the model with the poorest DIC out of all models for all nine
 365 participants.

366 ν -nonlinear-ERP

367 Posterior predictive data for the ν -nonlinear-ERP are shown in Figure 8. Visual
 368 inspection of the figure shows that the ν -nonlinear-ERP model fits both types of data well,
 369 although not as well as the ν -ERP model: ν -ERP has an average DIC across participants of
 370 31,880.75, whereas ν -nonlinear-ERP has an average DIC across participants of 31,910.22.
 371 Within participants, the ν -ERP model was DIC-preferred for 6 out of 9 people. For the
 372 remainder of the results section, we will examine the results of ν -ERP, the best of the
 373 models we have investigated, in more detail.

374 *Central Findings*

375 In sum, we find that of the models we considered, evidence for mean drift rate ν being
 376 the linking parameter between behavioral and neural data is strongest. Furthermore, we
 377 find that the relationship between mean drift rate ν and the neural data is linear in nature
 378 (though for some participants, a nonlinear link provides a better account of the data).

379 To highlight the central research findings, we will now examine effects across condi-
 380 tions. Summarized data are displayed in Figure 9, with corresponding summaries from the

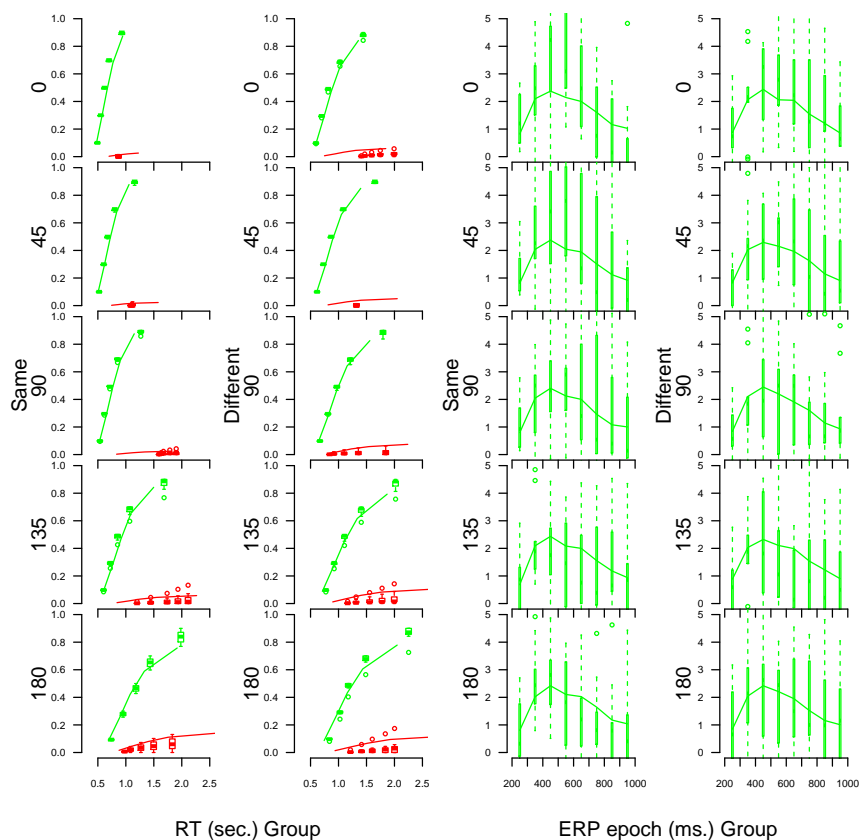


Figure 6. Posterior predictive data show that the t_0 -ERP model fits the behavioral data well, and the neural data comparatively poorly. Left two columns: proportion correct (y-axis) plotted against RTs (x-axis) for the .1, .3, .5, .7, and .9 quantiles calculated from correct RTs (green) and error RTs (red). Right two columns: mean ERP amplitudes in negative microvolts (y-axis) for eight different time windows (x-axis). For all panels, boxplots represent empirical data and lines represent posterior predictive data.

381 posterior predictions of the best-supported joint model, ν -ERP. The top-left panel displays
 382 median RTs for different conditions and stimulus types. RT steadily increases as the rota-
 383 tion angle increases, and also median RT is higher for “different” stimuli than for “same”
 384 stimuli. The model captures both of these data patterns very accurately. The bottom-left
 385 panel displays mean proportion of correct decisions, separately for different conditions and
 386 stimulus types. Accuracy drops as the rotation angle increases, though the trend is less
 387 clear than for RTs. The bottom-left panel confirms the earlier observation that the model
 388 underestimates some of the accuracies.

389 The top-right panel displays ERPs for each 100 ms epoch from 200ms up to 1,000ms
 390 for “same” stimuli. The amplitude of the ERPs drops as the rotation angle increases. Given
 391 the size of the error bars (displayed in the far right of the panel), the mismatch between
 392 the data and the model is modest. The bottom-right panel displays ERPs for each 100 ms

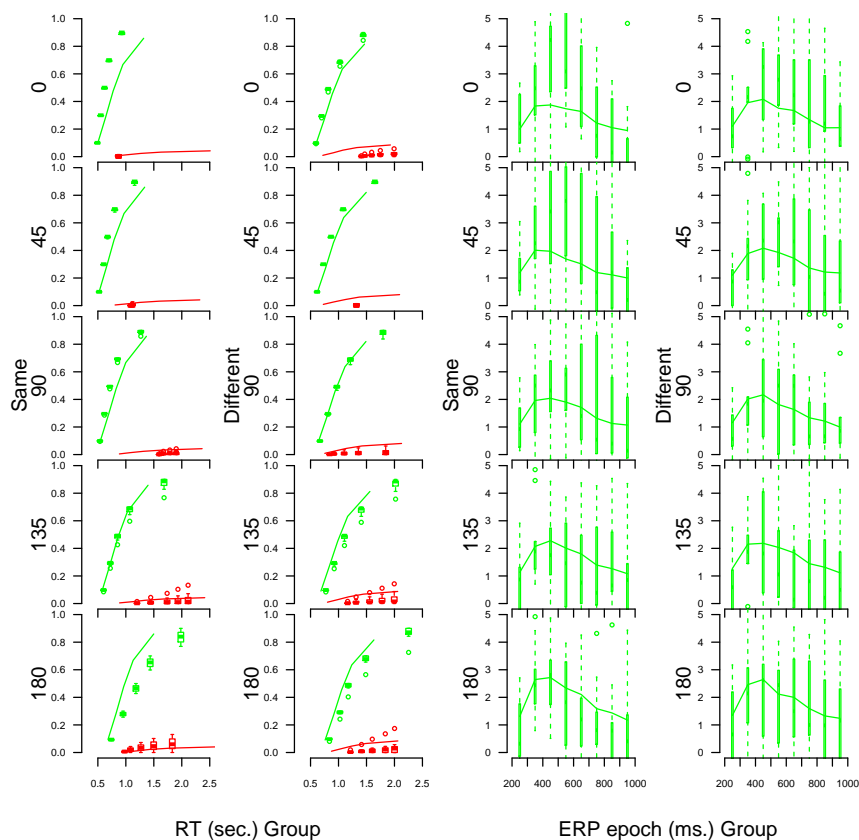


Figure 7. Posterior predictive data show that the *Brev- t_0 -ERP* model fits both the behavioral and the neural data quite poorly. Left two columns: proportion correct (y-axis) plotted against RTs (x-axis) for the .1, .3, .5, .7, and .9 quantiles calculated from correct RTs (green) and error RTs (red). Right two columns: mean ERP amplitudes in negative microvolts (y-axis) for eight different time windows (x-axis). For all panels, boxplots represent empirical data and lines represent posterior predictive data.

epoch from 200 up to 1,000ms for “different” stimuli. Again, the amplitude of the ERPs drops as the rotation factor increases, though interestingly the ERPs for 135° and 180° have reversed order. The model captures the data well, as can be observed by comparing the modest mismatch between data and model to the averaged error bars displayed in the far right of the panel.

The bottom-right panel also includes medians of the posterior distribution over the group level linking parameter (β), with error bars capturing the central 50% of the distribution. The size of linking parameter β follows the amplitude of the rotation-angle effects in the ERP data. To reiterate, estimates of the linking parameter provide time-sensitive measures of the link between behavioral and neural data. For example, at each time window the different rotation angles lead to different ERP measurements (the colored dots vertically spaced), with some time windows showing very little differences between angles and some

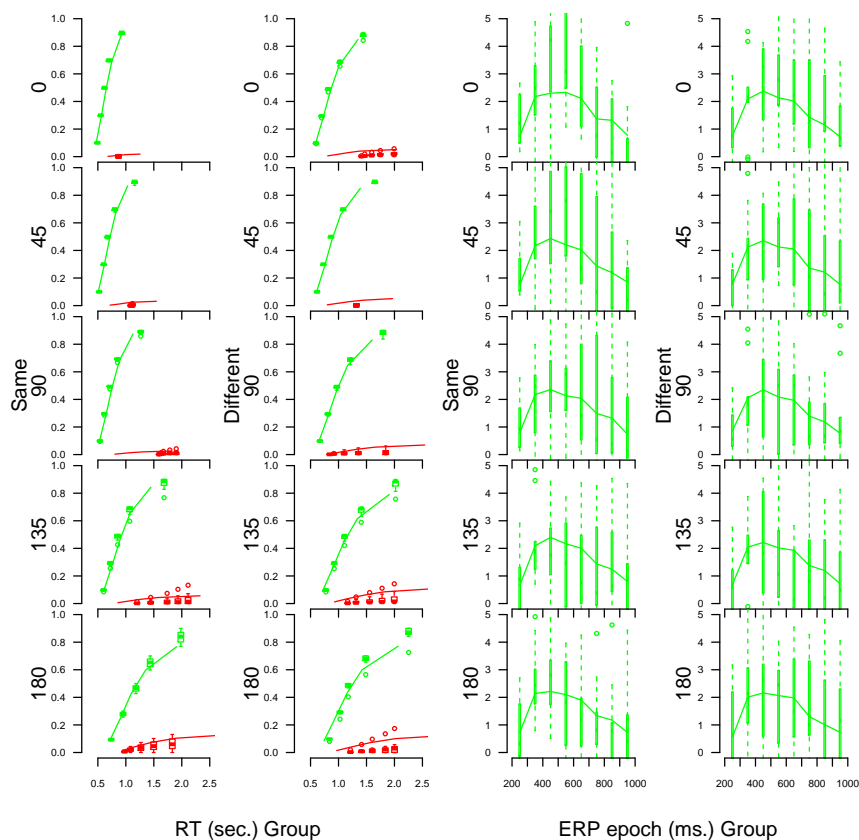


Figure 8. Posterior predictive data show that the ν -nonlinear-ERP model fits the behavioral data well, and the neural data comparatively poorly. Left two columns: proportion correct (y -axis) plotted against RTs (x -axis) for the .1, .3, .5, .7, and .9 quantiles calculated from correct RTs (green) and error RTs (red). Right two columns: mean ERP amplitudes in negative microvolts (y -axis) for eight different time windows (x -axis). For all panels, boxplots represent empirical data and lines represent posterior predictive data.

405 showing very large differences. The model captures these effects, even though the linking
 406 function and linking parameters are identical for all angle conditions. This happens because
 407 the drift rates are estimated differently for the different angle conditions (and for same vs.
 408 different stimulus classes), and these different drift rates influence the ERP predictions via
 409 the linking function.

410

Conclusion

411 This paper provided an example for cognitive scientists who are interested in in-
 412 vestigating the correspondence between neural and behavioral data via building computa-
 413 tional models for both data streams. We compared four different models that differ in the
 414 parametrization on the behavioral level and in the linking assumptions and showed that
 415 drift rate is capable of simultaneously explaining the behavioral data and the neural data.

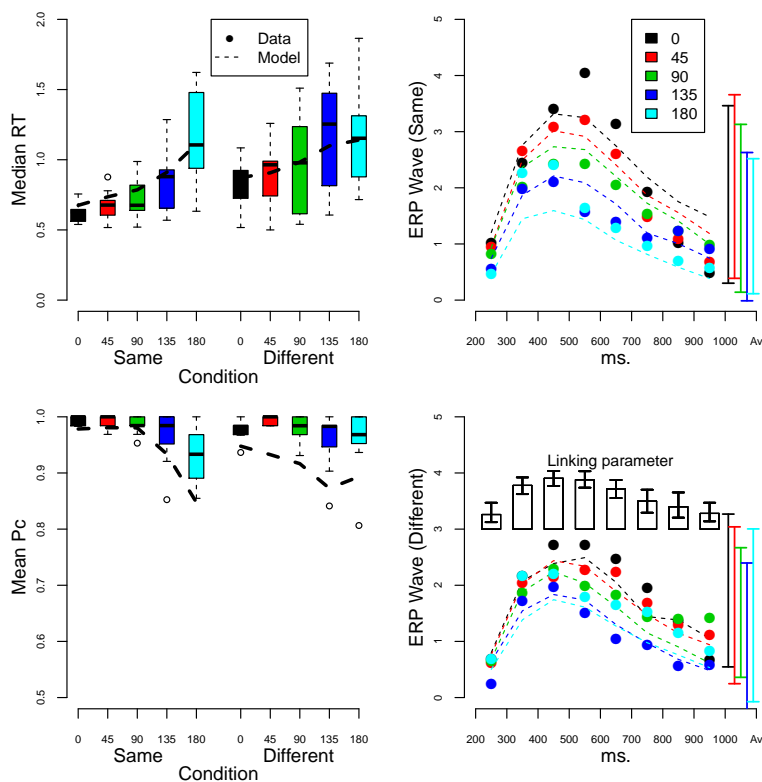


Figure 9. Behavioral and neural data, displayed for each stimulus type and angle condition. Top-left panel: Boxplots display median RT for participants in seconds. Bottom-left panel: Boxplots display proportion correct for participants. Right panels: ERPs in negative microvolts. The far right of both panels display error bars, averaged over all time slots. Inset for the bottom-right panel shows linking parameter β displayed for each time slot with error bars. Error bars in the right panels represent the central 50% of the distribution.

416 The joint modeling approach that we have used relies on the precise instantiation
 417 of hypotheses about the links between parameters related to neural data and parameters
 418 related to behavioral data. In addition to specifying which parameters are linked, this
 419 approach also requires specification of a particular linking function. The different model
 420 versions we investigated differed in these elements, and provided a rigorous framework for
 421 investigating important theoretical questions. For example, our model comparisons revealed
 422 that, for most participants at least, a simple linear link between drift rate and average ERP
 423 amplitude was better than a sigmoidal link. Similarly, an explanation of rotation angle
 424 effects in both behavioral and neural data was better when based on drift rates than on
 425 non-decision time. It is, of course, entirely conceivable that both drift rate and non-
 426 decision time play a role in linking behavioral data to ERP data (recall that DIC preferred
 427 the ν -ERP model over the t_0 -ERP model for most, but not all, participants). Provost and
 428 Heathcote (2015) explored more sophisticated models using a sequential, two-stage process,
 429 to separate the decision process from the mental rotation process. In Provost et al.'s account,

430 the decision processing is delayed by a random amount of time taken to mentally rotate the
431 stimulus, which is equivalent to assuming a random distribution for the non-decision time
432 (t_0) in our model. Provost et al.’s analyses supported models with variable non-decision
433 time processes, and in particular those where the variability increased with the mean. An
434 interesting avenue for future research would be to extend the various model comparisons
435 we have made (above) to models with sophisticated random distributions for non-decision
436 time.

437 Our approach to linking neural and behavioral data is not unique, and is not necessar-
438 ily the best for many different situations. Still, we propose that, when possible, researchers
439 should strive for the tightest possible linking, as this provides the greatest opportunity to
440 investigate the underlying linking assumptions. Put differently, joint models that are tightly
441 linked allow us to uncover underlying psychological processes that simultaneously explain
442 behavioral and neural data. Such an approach is arguably more powerful than more loosely
443 linked models, which often do not go beyond correlations between different levels of data.
444 The “when possible” caveat relates to the state-of-the-art in the cognitive modeling and
445 neural modeling of the research field in question. Very tightly-linked models, with explicit
446 and quantitative linking assumptions, are only possible in research fields with tractable
447 quantitative models for both behavioral and neural data.

448 One of the more interesting implications of joint modeling is trying to relate two
449 streams of data with potentially vastly different scales. In our particular example, we are
450 combining RT data in seconds (from 0 to 7), proportion correct (from 0 to 1), and mean
451 amplitudes at Pz (90% fall in the range -7.5 to 11). Revealing how the different kinds of
452 model misfit interact, and how much influence they have relative to one another, is another
453 of the strengths of the joint modeling approach we have used. Direct comparison of the
454 fits of model that vary in just one component can be very revealing about that component
455 (conditional on the other model components being reasonable, of course). For instance,
456 our models ν -ERP and t_0 -ERP differed only on the neural linking component, whereas
457 t_0 -ERP and *Brev*- t_0 -ERP differed only on the behavioral component, and these pairings
458 allowed us to investigate interesting psychological questions.

459 Our example model demonstrates a very tight link between neural and behavioral data
460 in the field of simple decision-making. This field has seen some excellent interdisciplinary
461 work between neuroscience and psychology (e.g. Purcell et al., 2010). The example model
462 we developed shows how to adapt the LBA model for response time data to incorporate
463 ERP data, recorded during a mental rotation task. The result is a joint model that can
464 simultaneously capture characteristics of data at the behavioral level (response times and
465 choice proportions) and the neural level (ERPs). Approaches like this are very exciting,
466 because they help to reduce barriers between two fields that have operated alongside another
467 rather than together for a long time. We hope that modeling data at different levels with
468 a single set of parameters paves the way to a more integrative cognitive science.

References

469

- 470 Anderson, J. R., & Fincham, J. M. (2014). Discovering the sequential structure of thought. *Cognitive*
 471 *Science*, *38*, 322–352.
- 472 Atkinson, R. C., & Shiffrin, R. M. (1968). Human memory: A proposed system and its control
 473 processes. *Psychology of Learning and Motivation*, *2*, 89–195.
- 474 Belliveau, J., Kennedy, D., McKinstry, R., Buchbinder, B., Weisskoff, R., Cohen, M., ... Rosen,
 475 B. (1991). Functional mapping of the human visual cortex by magnetic resonance imaging.
 476 *Science*, *254*, 716–719.
- 477 Brenner, D., Williamson, S., & Kaufman, L. (1975). Visually evoked magnetic fields of the human
 478 brain. *Science*, *190*, 480–482.
- 479 Brown, S., & Heathcote, A. (2008). The simplest complete model of choice reaction time: Linear
 480 ballistic accumulation. *Cognitive Psychology*, *57*, 153–178.
- 481 Forstmann, B., Dutilh, G., Brown, S., Neumann, J., von Cramon, D., Ridderinkhof, K., & Wagen-
 482 makers, E.-J. (2008). Striatum and pre-SMA facilitate decision-making under time pressure.
 483 *Proceedings of the National Academy of Sciences*, *105*, 17538–17542.
- 484 Gamerman, D., & Lopes, H. F. (2006). *Markov chain Monte Carlo: Stochastic simulation for*
 485 *Bayesian inference*. Boca Raton, FL: Chapman & Hall/CRC.
- 486 Gilks, W. R., Richardson, S., & Spiegelhalter, D. J. (Eds.). (1996). *Markov chain Monte Carlo in*
 487 *practice*. Boca Raton (FL): Chapman & Hall/CRC.
- 488 Gold, J. I., & Shadlen, M. N. (2007). The neural basis of decision making. *Annual Review of*
 489 *Neuroscience*, *30*, 535–574.
- 490 Hanes, D. P., & Schall, J. D. (1996). Neural control of voluntary movement initiation. *Science*, *274*,
 491 427–430.
- 492 Heil, M. (2002). The functional significance of ERP effects during mental rotation. *Psychophysiology*,
 493 *43*, 401–412.
- 494 Hillyard, S. A., Hink, R. F., Schwent, V. L., & Picton, T. W. (1973). Electrical signs of selective
 495 attention in the human brain. *Science*, *182*, 177–180.
- 496 Ho, T. C., Brown, S., Abuyo, N. A., Ku, E.-H. J., & Serences, J. T. (2012). Perceptual consequences
 497 of feature-based attentional enhancement and suppression. *Journal of vision*, *12*, 1–17.
- 498 Ho, T. C., Brown, S., & Serences, J. T. (2009). Domain general mechanisms of perceptual decision
 499 making in human cortex. *The Journal of Neuroscience*, *29*, 8675–8687.
- 500 Lee, M. D., & Wagenmakers, E.-J. (2013). *Bayesian cognitive modeling: A practical course*.
 501 Cambridge University Press. Retrieved from <http://books.google.com.au/books?id=Gq6kAgAAQBAJ>
 502
- 503 Lewandowsky, S., & Farrell, S. (2010). *Computational modeling in cognition: Principles and practice*.
 504 Sage.
- 505 Link, S. W., & Heath, R. A. (1975). A sequential theory of psychological discrimination. *Psychome-*
 506 *trika*, *40*, 77–105.
- 507 Luce, R. D. (1986). *Response times*. New York: Oxford University Press.
- 508 Nosofsky, R. M. (1986). Attention, similarity, and the identification–categorization relationship.
 509 *Journal of Experimental Psychology: General*, *115*, 39–57.
- 510 Nosofsky, R. M., & Palmeri, T. J. (1997). An exemplar–based random walk model of speeded
 511 classification. *Psychological Review*, *104*, 266–300.
- 512 Pouget, P., Logan, G. D., Palmeri, T. J., Boucher, L., Paré, M., & Schall, J. D. (2011). Neural
 513 basis of adaptive response time adjustment during saccade countermanding. *The Journal of*
 514 *Neuroscience*, *31*, 12604–12612.
- 515 Provost, A., & Heathcote, A. (2015). Titrating decision processes in the mental rotation task.
 516 *Psychological Review*, *122*, 735–754.
- 517 Provost, A., Johnson, B., Karayanidis, F., Brown, S. D., & Heathcote, A. (2013). Two routes to
 518 expertise in mental rotation. *Cognitive Science*, *37*, 1321–1342.

- 519 Purcell, B. A., Heitz, R. P., Cohen, J. Y., Schall, J. D., Logan, G. D., & Palmeri, T. J. (2010).
520 Neurally constrained modeling of perceptual decision making. *Psychological Review*, *117*,
521 1113–1143.
- 522 Raaijmakers, J. G. W., & Shiffrin, R. M. (1981). Search of associative memory. *Psychological*
523 *Review*, *88*, 93–134.
- 524 Rae, B., Heathcote, A., Donkin, C., Averell, L., & Brown, S. D. (2014). The hare and the tortoise:
525 Emphasizing speed can change the evidence used to make decisions. *Journal of Experimental*
526 *Psychology: Learning, Memory, and Cognition*, *40*, 1226–1243.
- 527 Ratcliff, R. (1978). A theory of memory retrieval. *Psychological Review*, *85*, 59–108.
- 528 Riečanský, I., & Jagla, F. (2008). Linking performance with brain potentials: Mental rotation-
529 related negativity revisited. *Neuropsychologia*, *46*, 3069–3073.
- 530 Schall, J. D. (2001). Neural basis of deciding, choosing, and acting. *Nature Reviews Neuroscience*,
531 *2*, 33–42.
- 532 Shadlen, M. N., & Newsome, W. T. (1996). Motion perception: Seeing and deciding. *Proceedings*
533 *of the National Academy of Sciences*, *93*, 628–633.
- 534 Shepard, R. N., & Metzler, J. (1971). Mental rotation of three-dimensional objects. *Science*, *171*,
535 701–703.
- 536 Spiegelhalter, D. J., Best, N. G., Carlin, B. P., & van der Linde, A. (2002). Bayesian measures of
537 model complexity and fit. *Journal of the Royal Statistical Society B*, *64*, 583–639.
- 538 Sutton, S., Braren, M., Zubin, J., & John, E. (1965). Evoked-potential correlates of stimulus
539 uncertainty. *Science*, *150*, 1187–1188.
- 540 Teller, D. (1984). Linking propositions. *Vision Research*, *24*, 1233–1246.
- 541 Trueblood, J. S., Brown, S. D., & Heathcote, A. (2014). The multiattribute linear ballistic ac-
542 cumulator model of context effects in multialternative choice. *Psychological Review*, *121*,
543 179–205.
- 544 Turner, B. M., Forstmann, B. U., Love, B. C., Palmeri, T. J., & van Maanen, L. (in press).
545 Approaches to analysis in model-based cognitive neuroscience. *Journal of Mathematical Psy-*
546 *chology*.
- 547 Turner, B. M., Forstmann, B. U., Wagenmakers, E.-J., Brown, S. D., Sederberg, P. B., & Steyvers,
548 M. (2013). A Bayesian framework for simultaneously modeling neural and behavioral data.
549 *Neuroimage*, *72*, 193–206.
- 550 Turner, B. M., Sederberg, P. B., Brown, S. D., & Steyvers, M. (2013). A method for efficiently
551 sampling from distributions with correlated dimensions. *Psychological Methods*, *18*, 368–384.
- 552 Usher, M., & McClelland, J. L. (2001). On the time course of perceptual choice: The leaky competing
553 accumulator model. *Psychological Review*, *108*, 550–592.
- 554 van Ravenzwaaij, D., Cassey, P., & Brown, S. D. (in press). A simple introduction to Markov Chain
555 Monte-Carlo. *Psychonomic Bulletin & Review*.
- 556 Wagenmakers, E.-J. (2009). Methodological and empirical developments for the Ratcliff diffusion
557 model of response times and accuracy. *European Journal of Cognitive Psychology*, *21*, 641–
558 671.